Resolution of the Thomson spectrometer

R. F. Schneider, C. M. Luo, and M. J. Rhee
Laboratory for Plasma and Fusion Energy Studies, University of Maryland, College Park, Maryland 20742

(Received 13 March 1984; accepted for publication 24 July 1984)

The resolution of Thomson spectrometers is examined. Charge, mass energy, and momentum resolutions are found as functions of collimation parameters and field strengths. The results are generally applicable to all Thomson spectrometer systems. In conjunction with this analysis, a compact Thomson spectrometer with high resolving power is described.

I. INTRODUCTION

Thomson spectrometers have recently been widely used for the analysis of ion beams produced in collective ion acceleration[1–6] and plasma focus[7–11] experiments. They are found extremely useful for the investigation of ion sources in any device that produces a beam of sufficient intensity or duration compatible with the large degree of collimation necessary for this device. Recently we reported[12] the construction of a Thomson spectrometer which utilizes the highly sensitive nuclear track plate known as CR-39 as a detector and a small permanent magnet. The use of this highly sensitive detector allows a high degree of collimation of the beam in order to produce a compact Thomson spectrometer with high resolving power. The methods by which ion species and energy spectra are obtained from the raw data on the detector are discussed in Ref. 12. In this paper, we will analyze the factors which affect the resolution of the Thomson spectrometer and apply them to the newly constructed compact Thomson spectrometer which has much higher resolving power.

II. DETECTOR IMAGE GEOMETRY

The compact Thomson spectrometer geometry which employs the second collimating pinhole downstream of the field region leads to a simplification in the treatment of the Thomson spectrogram. In the following, we employ a small angle approximation by setting tan θ equal to θ. This introduces an error on the order of 1.5% for deflection angles of 200 mrad or less. This approximation introduces much less error than other factors which we shall consider, and is in fact commonly used in Thomson spectrometer analysis. The magnetic and electric deflections on the detector, x_m and x_e, are proportional to the magnetic and electric deflection angles, θ_m and θ_e, by

$$\theta_i = x_i/L, \tag{1}$$

where L is the distance from the downstream (second) pinhole to the detector in the compact spectrometer (L_2 in Fig. 1). This analysis may also be applied to conventional Thomson spectrometers which utilize both collimating pinholes upstream of the field region. It is necessary in this case to define L as the distance from the detector to the point where incident and final particle trajectories intersect. Usually, this is taken to be the center of the field region. The magnetic and electric deflection angles, θ_m and θ_e, are given by the simple nonrelativistic expressions:

$$\theta_m = \frac{Ze\int Bdl}{p}, \tag{2}$$

$$\theta_e = \frac{Ze\int Edl}{2T}, \tag{3}$$

where Ze is the product of ion charge state and electronic charge, $\int Bdl$ and $\int Edl$ are the integrals of the magnetic and electric fields along the ion path length, and T and p are the ion energy and momentum respectively. MKS units are used throughout. By elimination of p and T, Eqs. (2) and (3) combine to give the well-known parabola equation:

$$\theta_m^2 = \frac{Z}{A}\left(\frac{e}{u}\frac{\left(\int Bdl\right)^2}{\left(\int Edl\right)}\right)\theta_e, \tag{4}$$

where A is the atomic mass number of the ion, and u is the unit mass of a nucleon, 1.66×10^{-27} kg.

A major purpose of the Thomson spectrometer is to separate parabolas of different charge to mass ratio in order to differentiate ion species and charge state. This, in principle, happens naturally if the parabola is an infinitely thin line. Practically, however, this can never be done since the collimation procedure utilizes two pinholes which produce an image with a finite diameter as displayed in Fig. 1. The resulting width of the parabolas, which are swept out by the different energies of a given charge to mass ratio, leads to overlapping, which reduces the resolution of the spectrometer. From the geometry of Fig. 1, the width of the parabola on the detector is given by

$$D_3 = \frac{L_2}{L_1}(D_1 + D_2) + D_2. \tag{5}$$

This corresponds to a subtended angle of

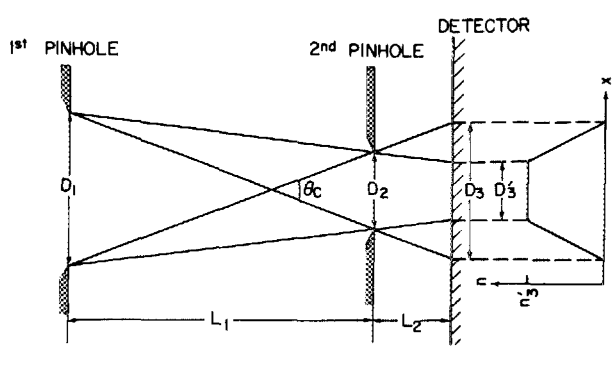

FIG. 1. Detector image geometry showing density profile and spot sizes given by Eqs. (5) and (21).

 0021-8979/85/010001-05$02.40

$$\delta = \frac{D_3}{L}. \quad (6)$$

As in Eq. (1), L here is different for conventional and compact spectrometers. The overlapping of the parabolas as they near the origin can be calculated and resolution criterion can be obtained by determining the points where different charge-to-mass ratio parabolas are separated for either constant charge or constant mass. It is interesting to note that these equations arise solely from the pinhole geometry and are independent of the location of the field region, hence this analysis is completely general. The only difference between compact and conventional spectrometers is the position of the pinholes relative to the fields. In the compact spectrometer, the field region is placed between the first and second pinholes allowing much more control over the diameter of the pinhole collimation image on the detector. In conventional spectrometers, the pinhole collimation system is entirely upstream of the fields. This implies that the distance L_2 in Fig. 1 must be large enough to contain the fields. This limits the minimum obtainable D_3, and hence requires a spectrometer which is an order of magnitude larger to obtain the same resolution.

III. CHARGE AND MASS RESOLUTION ANALYSIS

To analyze charge resolution, we suppose we have one ion species with several different charge states. Along what curve can we find the points at which neighboring parabolas are separated? To answer, we use the criterion for separation that $\Delta\theta_m$, the separation of the centers of the parabolas along a vertical line, i.e., θ_m direction, must be greater than the parabola width along that line,

$$\Delta\theta_m \geqslant \delta\left(1+\frac{\theta_m^2}{4\theta_e^2}\right)^{1/2} \text{ and } \Delta\theta_e = 0. \quad (7)$$

This is illustrated in Fig. 2. Here we have made use of the fact that the slope of the parabola is given by

$$\frac{d\theta_m}{d\theta_e} = \frac{\theta_m}{2\theta_e}, \quad (8)$$

which is derived from the parabola Eq. (4). Assuming small $\Delta\theta_m$, we can substitute the separation condition Eq. (7) into the total differential of the parabola Eq. (4) with Z, A, θ_e, and θ_m as variables yielding

$$\frac{dZ}{A} - Z\frac{dA}{A_2} = \frac{u}{e}\frac{\int Edl}{\left(\int Bdl\right)^2}\frac{2\theta_m}{\theta_e}\delta\left[1+\left(\frac{\theta_m}{2\theta_e}\right)^2\right]^{1/2}. \quad (9)$$

If $dA = 0$ and $dZ = 1$, we will arrive at the equation describing the line connecting the points of charge resolution for a certain ion species:

$$\theta_m^4 + \theta_m^2(4\theta_e^2) - \left(\frac{k}{A\delta}\right)^2\theta_e^4 = 0 \quad (10)$$

We have made the definition

$$k = \frac{e}{u}\frac{\left(\int Bdl\right)^2}{\int Edl}. \quad (11)$$

The physical solution to the quartic equation is

$$\theta_m = \left\{\left[4+\left(\frac{k}{A\delta}\right)^2\right]^{1/2} - 2\right\}^{1/2}\theta_e, \quad (12)$$

which describes a straight line which intersects the origin with slope $\{[4+(k/A\delta)^2]^{1/2}-2\}^{1/2}$. This is illustrated in Fig. 3. Below this line, the parabolas of every charge state of ion mass A are separated. An alternate way of viewing this is to note that such lines are constant velocity lines with velocity $v = (\int Edl/\int Bdl)\{[4+(k/A\delta)^2]^{1/2}-2\}^{1/2}$. Any ions with velocity less than this value will be resolved. Thus, large values of k/δ will yield better charge resolution.

For mass resolution, let $dZ = 0$, $dA = 1$:

$$-\frac{Z}{A^2} = \frac{1}{k}\frac{2\theta_m}{\theta_e}\delta\left[1+\left(\frac{\theta_m}{2\theta_e}\right)^2\right]^{1/2}. \quad (13)$$

Using Eq. (4) to eliminate A, we obtain

$$\theta_m^6 - (Zk\delta\theta_m)^2 - 4(Zk\delta\theta_e)^2 = 0, \quad (14)$$

which can be solved numerically. An interesting analytical result can be derived when the charge state Z in Eq. (13) is eliminated in favor of mass number A. In this case, we find

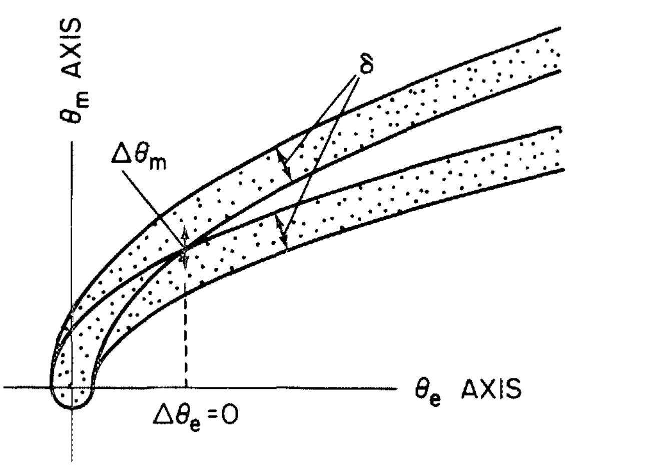

FIG. 2. Simulated Thomson spectrogram showing geometry of parabola separation with finite parabola width. The condition for separation of the parabolas is given by Eq. (7).

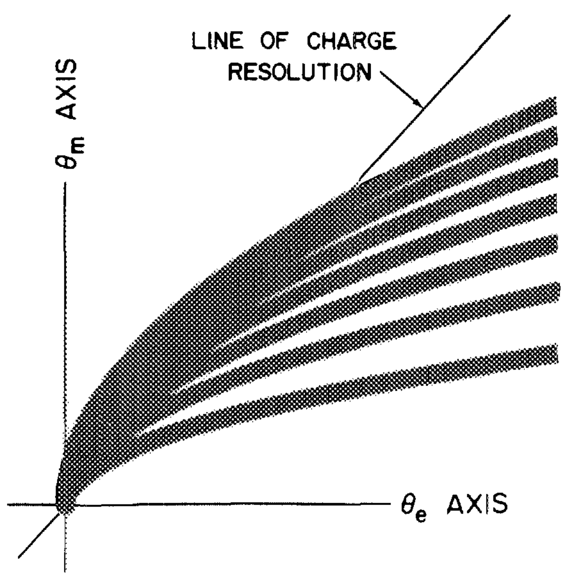

FIG. 3. Charge resolution geometry. Shown is a set of parabolas with $A = 35$, $k = 1.00$, and $\delta = 11$ mrad. The line of charge resolution is calculated from Eq. (12).

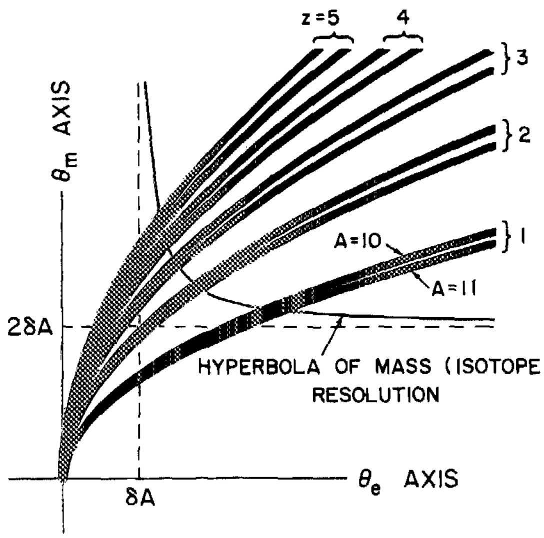

FIG. 4. Mass (isotope) resolution geometry. Resolution curves that describe points of separation of parabolas corresponding to mass numbers A and $A+1$ at different charge states are described by hyperbolas with asymptotes at $\theta_e = A\delta$ and $\theta_m = 2A\delta$. Shown is $\delta = 5.5$ mrad and $A = 10$.

the line which connects the resolution points (points of separation) of parabolas with atomic numbers A and $A+1$ with different charge states:

$$\theta_m = \frac{2A\delta\theta_e}{[\theta_e^2 - (A\delta)^2]^{1/2}}. \tag{15}$$

This equation describes a hyperbola with asymptotes $\theta_e = A\delta$ and $\theta_m = 2A\delta$ above which isotopes are resolved as in Fig. 4. This can be generalized to $dA = n$ provided $n/A \ll 1$ in order to obtain a resolution curve for elements which differ in mass number by n. This leads to the simple modification in Eq. (15) that A must be replaced by A/n everywhere it appears.

IV. ANALYSIS OF ENERGY AND MOMENTUM RESOLUTION

Energy and momentum resolution is also limited by the subtended angle of the pinhole collimation spot δ. The spectrogram can be thought of as a superposition of many of these spots infinitely close together along the parabola. Energy or momentum, which is found from either the electric or magnetic deflection angle is hence uncertain by an amount corresponding to the projection of the collimation spot length δ along the parabola onto the electric or magnetic axis of the spectrogram [see Fig. 5(a)]. Within our approximation, these quantities are related by the equation

$$\delta^2 = \left[1 + \left(\frac{\theta_m}{2\theta_e}\right)^2\right](\Delta\theta_e)^2, \tag{16}$$

where we have used Eq. (8). Relative energy and momentum uncertainties $\Delta T/T$ and $\Delta p/p$ can be found from the deflection Eqs. (2) and (3) in terms of θ_e as

$$\alpha_T = \frac{\Delta T}{T} = -\frac{\Delta\theta_e}{\theta_e},$$
$$\alpha_p = \frac{\Delta p}{p} = -\frac{\Delta\theta_e}{2\theta_e}. \tag{17}$$

A quantity Q_i, representing either T or p can then be expressed along with its uncertainty as $Q_i(1 \pm \alpha_i/2)$. It is of interest to find the curves of constant α_i which will give a contour map of relative uncertainty of energy or momentum. Substitution of Eq. (17) into Eq. (16) yields

$$\frac{\theta_e^2}{\left(\frac{\delta}{\alpha_T}\right)^2} + \frac{\theta_m^2}{\left(\frac{2\delta}{\alpha_T}\right)^2} = 1,$$
$$\frac{\theta_e^2}{\left(\frac{\delta}{2\alpha_p}\right)^2} + \frac{\theta_m^2}{\left(\frac{\delta}{\alpha_p}\right)^2} = 1. \tag{18}$$

These describe upright ellipses about the origin which are contours of constant relative uncertainty as illustrated in Fig. 5(b). The relative energy or momentum resolution at a certain point on the parabola corresponds to the α_T or α_p value of the ellipse that intersects that point. In terms of spectrometer parameters, by combining Eqs. (2), (3), and (18)

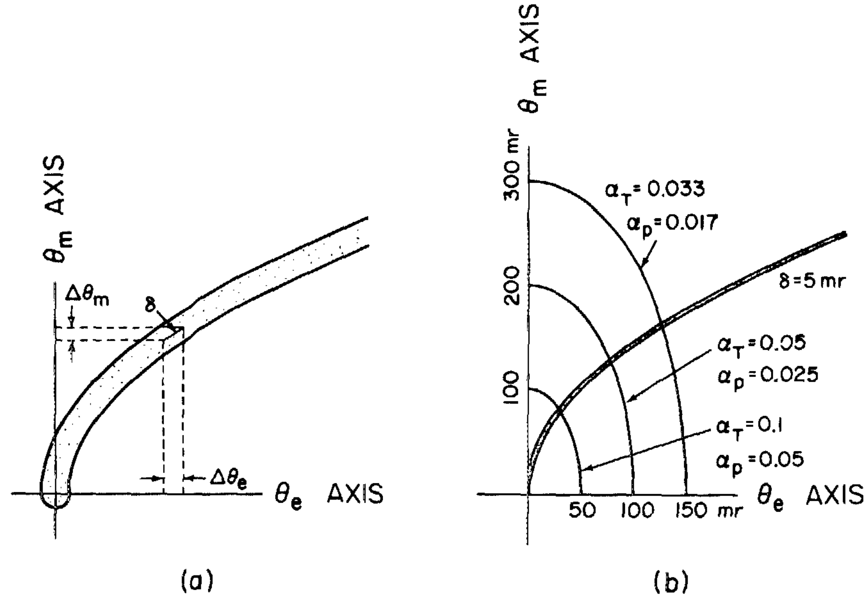

FIG. 5. (a) Energy or momentum, which is derived from projection on the θ_e or θ_m axis, is uncertain due to the spot size δ as it is projected onto the axes. (b) This uncertainty gives contours of constant relative energy or momentum uncertainty which are ellipses. Shown is a $\delta = 5$ mrad parabola with some associated contours.

with the definition of k, we can find the energy uncertainty of a certain ion species as a function of its energy per charge as

$$\alpha_T = \frac{2(T/Z)\delta}{e\int E dl}\left[1 + \left(\frac{Z}{A}\right)\frac{(T/Z)k}{2e\int E dl}\right]^{-1/2}, \quad (19)$$

or more simply, in terms of electric deflection angle θ_e,

$$\alpha_T = \frac{\delta}{\theta e}\left[1 + \frac{Z}{A}\left(\frac{k}{4\theta_e}\right)\right]^{-1/2}. \quad (20)$$

V. COMPARISON OF SPECTROMETERS

The principles examined in the previous sections are applied to the design of a new compact Thomson spectrometer in order to improve resolution over previously reported spectrometers.[4,6,11,12] Resolution analysis shows us the importance of the parameters k and δ. The lower limit of δ is determined by the ion flux produced by the source for the spectrometer. If one tries to make δ too small, insufficient flux will reach the detector to make the parabolas distinguishable or to provide enough statistical information to produce useful energy spectra. For maximum flux to reach the detector, D_3' in Fig. 1 must be larger than zero (nonnegative). D_3' is given by the equation

$$D_3' = \frac{L_2}{L_1}(D_2 - D_1) + D_2 > 0. \quad (21)$$

In conjunction with this consideration, we wish to make δ as small as possible. It has been discussed in Ref. 12 that simultaneously satisfying both conditions is best accomplished by placing the second pinhole in the collimation system downstream of the field region. The spectrometer is shown in Fig. 6. A single pinhole (not shown in Fig. 6) is placed approximately 40 cm upstream of the spectrometer. When the beam reaches the spectrometer after passing through the first pinhole, it is relatively diffuse and usually covers the entire spectrometer entrance area. This condition depends upon the nature of the ion source as well as its distance from the first (upstream) pinhole. Usually all plasma type sources are of satisfactory nature. Upon entering the spectrometer, the ion trajectories are parallel to each other and perpendicular to the fields. The ions passing through the field region are deflected and subsequently pass through the second (downstream) pinhole. The position they impact on the detector then depends only upon the velocity components they had upon leaving the pinhole. Experience shows that scattering from the pole pieces is not a problem.

The parameter k is proportional to the square of $\int Bdl$ and inversely proportional to $\int Edl$. The minimum value of $\int Edl$ is limited by the energy range of the ions to be analyzed as well as the acceptance angle of the magnetic pole gap. $\int Bdl$ is in general not limited in this manner and we are free to choose higher values of $\int Bdl$ in order to increase resolving power of the spectrometer. In order to obtain a large $\int Bdl$, the spectrometer is made from rare-earth cobalt 2.54-cm-diam disc magnets which are placed within a soft iron case. The pole gap used is 2.54 mm. The soft iron case provides good containment of the fields. $\int Bdl$ is found by Am^{241} α-particle calibration[5,12] to have the value 1.66×10^{-2} T m. The rare-earth cobalt magnets, which are insulated from the case, can be biased to high voltage producing the necessary E parallel to B configuration. $\int Edl$ is found experimentally to have the value $12.8 \times V$, where V is the voltage applied to the electrodes (magnets). Using typical values for this spectrometer, $\delta = 5.2$ mrad, $k = 1.48$, and $\int Edl = 1.80 \times 10^4$ V, from Eq. (19) we can obtain a plot of α_T, relative energy uncertainty, vs T/Z, energy per charge, for various charge to mass ratios (see Fig. 7). As in all Thomson spectrometer systems, the acceptance angle of the pole gap, the ion charge, and the electric field path integral, $\int Edl$, determine the minimum energy of the ions which may pass through the spectrometer

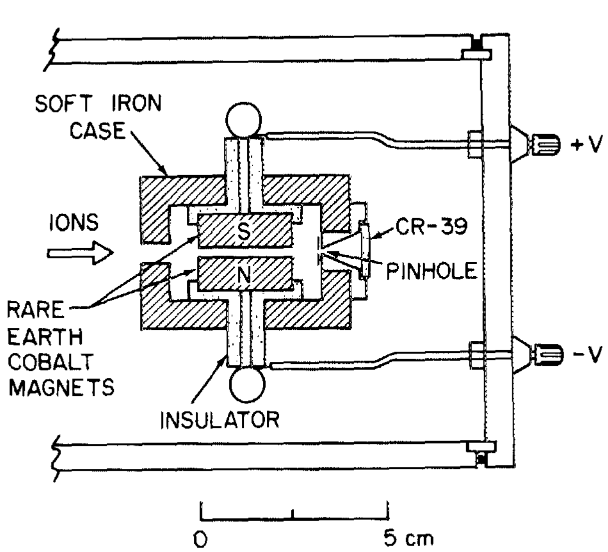

FIG. 6. Cross-sectional view of a high resolving power compact Thomson spectrometer.

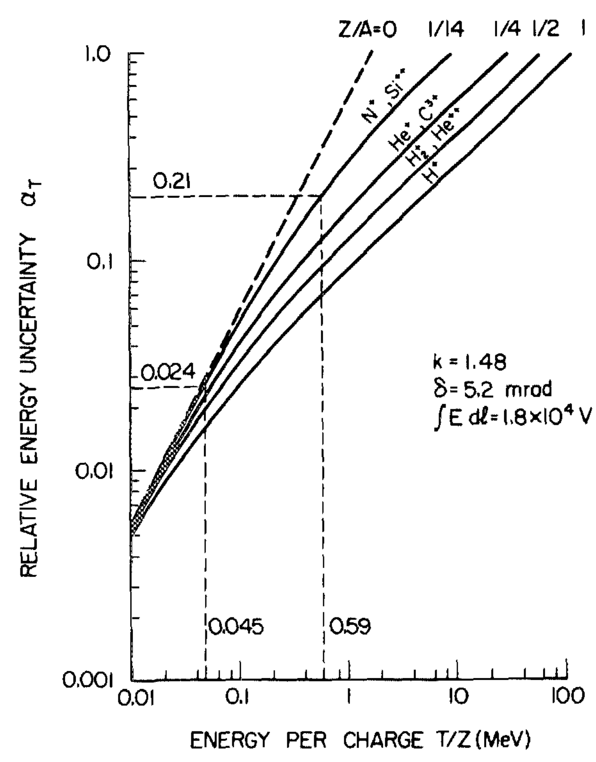

FIG. 7. Plot of relative energy uncertainty α_T vs energy per charge T/Z for several different charge to mass ratios and using the spectrometer parameters discussed in the text.

unobstructed by the pole pieces. For $\int E dl = 1.80\times10^4$ V, the minimum energy per charge which can be measured is 45 keV. For example, if we wish to analyze a N^+ parabola we see in Fig. 7 that the minimum possible relative energy uncertainty is 0.024 ($\pm$ 1.2%) for this spectrometer. A parabola obtained from a plasma focus ion source is shown in Fig. 8(b). The peak N^+ energy in Fig. 8(b) is 0.59 MeV which has a relative energy uncertainty α_T of 0.21 ($\pm$ 10.5%).

Spectrograms from both old and new spectrometers are obtained with a plasma focus device.[11] They are displayed in Fig. 8. Figure 8(a) shows a Thomson spectrogram with the parameters $\alpha = 6.0$ mrad and $k = 0.16$. The ions were identified as N^+, N^{2+}, and N^{3+}. From Eq. (12) we calculate the slope of charge resolution to be 0.87. This means that ions with velocity less than 3.2×10^6 m/s, or nitrogen kinetic energy, T_N, less than 740 keV, will be separated in charge. The two asymptotes for the hyperbola of mass resolution of Carbon ($A = 12$) and Oxygen ($A = 16$) from Nitrogen ($A = 14$) are shown on the spectrogram indicating that the region containing the tracks is not within the mass resolution region. In Fig. 8(b), δ is 5.2 mrad and k is now 1.48. The increased magnetic field brought the tracks into the mass resolution region enabling the identification of C and O impurities. The charge resolution region now contains the major portion of the mass resolution region. The charge resolution slope, 4.3, corresponds to a velocity of 4.7×10^6 m/s or T_N of 1.57 MeV.

We compare this spectrometer to one used for a collective ion acceleration experiment.[4,6] In this conventional spectrometer, both collimating pinholes are located upstream of the fields and are separated by 23 cm (L_1). The distance from the second (downstream) pinhole to the detector is 18.7 cm (L_2), and each pinhole is 0.2 mm in diameter. This yields a D_3 of 0.53 mm by Eq. (5). The distance from the center of the field region to the detector is 8.7 cm (L), hence by Eq. (6), $\delta = 6.0$ mrad. From the magnetic and electric field integrals of 9.48×10^{-3} T m and 3.42×10^4 V, respectively, we find $k = 0.25$. The slope of charge resolution for N is found from Eq. (12) to be 1.26, corresponding to a velocity of 4.55×10^6 m/s or $T_N = 1.50$ MeV. The asymptotes for mass resolution of C and O from N are $\theta_e = 42$ mrad and $\theta_m = 84$ mrad. This spectrometer has similar resolution to the one reported in this paper; however, its field region is an order of magnitude larger. This leads to larger spectrograms which are much more difficult to analyze quantitatively than small plates which can be viewed under a microscope.[12]

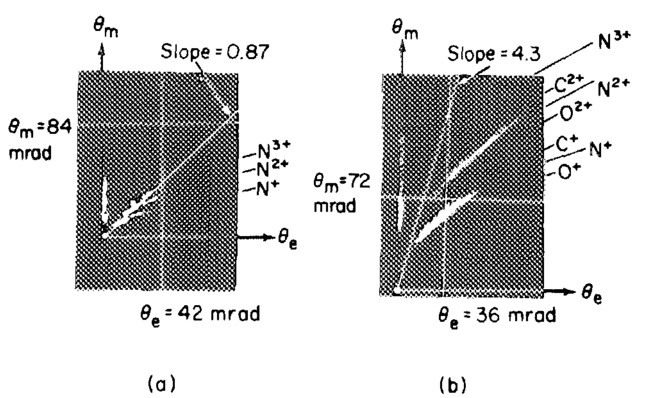

FIG. 8. Comparison of two spectrograms. (a) A Thomson spectrogram with $\delta = 6.0$ mrad and $k = 0.16$. The three lower parabolas were identified as N^+, N^{++}, and N^{3+}. The slope of charge resolution from Eq. (12) is 0.87. The asymptotes for resolution of C and O from N are $\theta_e = 42$ mrad and $\theta_m = 84$ mrad. (b) A spectrometer with higher resolving power separated the parabolas enabling the identification of carbon and oxygen impurities. For this spectrogram, $\delta = 5.2$ mrad and $k = 1.48$. The slope of charge resolution is 4.3. The asymptotes for resolution of C and O from N are $\theta_e = 36$ mrad and $\theta_m = 73$ mrad.

VI. CONCLUSIONS

The resolution of the Thomson spectrometer was examined, and simple analytic expressions for resolution curves were obtained. The importance of two parameters in particular was displayed, k and δ. In general, the ratio k/δ should be made as large as possible consistently with the ion energy range and the ion flux reaching the spectrometer. The analysis shows the advantages of the compact spectrometer design proposed by Rhee which places the second pinhole downstream of the field region. This design allows the reduction of δ without the associated sacrifice of ion track density on the detector. The energy range and acceptance angle of the pole gaps determines the optimum $\int E dl$. The new high resolving power Thomson spectrometer utilizes a permanent magnet with a much larger magnetic field increasing $\int B dl$ and hence k. The resulting spectrometer has applications in many fields of research.

ACKNOWLEDGMENTS

This work is supported by the Air Force Office of Scientific Research and the United States Department of Energy.

[1] G. W. Kuswa, L. P. Bradley, and G. Yonas, IEEE Trans. Nucl. Sci. **NS-20**, 305 (1973).

[2] R. F. Hoeberling, R. B. Miller, D. C. Straw, and D. N. Payton III, IEEE Trans. Nucl. Sci. **NS-24**, 1662 (1977).

[3] S. Takeda, M. Tamura, T. Yamamoto, and M. Kowanishi, Jpn. J. Appl. Phys. **18**, 641 (1979).

[4] W. W. Destler and J. T. Cremer, J. Appl. Phys. **54**, 636 (1983).

[5] J. R. Smith, Ph. D. Thesis, North Carolina State University, 1983.

[6] J. T. Cremer, Ph.D. Thesis, University of Maryland, 1984.

[7] M. J. Rhee, Bull. Am. Phys. Soc. **25**, 958 (1980).

[8] H. Herold, A. Mozer, M. Sadowski, and H. Schmidt, Rev. Sci. Instrum. **52**, 24 (1981).

[9] M. J. Rhee, IEEE Trans. Nucl. Sci. **NS-28**, 2663 (1981).

[10] A. Mozer, M. Sadowski, H. Herold, and H. Schmidt, J. Appl. Phys. **53**, 2959 (1982).

[11] M. J. Rhee and R. F. Schneider, IEEE Trans. Nucl. Sci. **NS-30**, 3192 (1983).

[12] M. J. Rhee, Rev. Sci. Instrum. **55**, 1229 (1984).